

2D simulation of leakage and damaged stability of oil carrier by MPS method

Simulação em 2D da estabilidade de um navio petroleiro avariado e do derramamento de óleo pelo método de MPS

Simulación en 2D de la estabilidad de un buque petroleo dañado y del derrame de petróleo por el método de MPS

Liang-Yee Cheng
Diogo Vieira Gomes
Kazuo Nishimoto

Abstract

This study carried out numerical simulations of the coupled transient processes of the oil leakage or water flooding and analyzed the stability of a damaged crude oil carrier. The numerical approach based on Moving Particle Semi-Implicit (MPS) method was applied to assess the dynamics of a two dimensional reduced scaled model and the oil-water multiphase flow with free surface. The results were compared with the stability analysis software SSTab, which provided the final list angle, and showed good agreement. In addition to the oil leakage and water flooding dynamics, which provide important information such as time from the breakdown to final list, the study's results also show the limits of the quasi-static approach.

keywords: ■ coupled analysis ■ oil leak ■ particle method ■ damaged stability ■ multiphase flow ■ MPS

Resumo

Este estudo realizou simulações numéricas dos processos transitórios e acoplados do derramamento de óleo ou inundação de água e analisou a estabilidade de um navio petroleiro avariado. A abordagem numérica baseada no método *Moving Particle Semi-Implicit* (MPS) foi aplicada para determinar a dinâmica de um modelo bidimensional em escala reduzida e o escoamento multifásico de óleo-água com superfície livre. Os resultados foram comparados com o *software* de análise de estabilidade SSTab, que forneceu o ângulo de adernamento final, e mostrou boa concordância. Além das dinâmicas de vazamento de óleo e da inundação de água, que fornecem informações importantes, tais como o tempo desde a danificação até a adernação final, os resultados do estudo mostram também os limites da abordagem quase-estática.

palavras-chave: ■ análise acoplada ■ vazamento de óleo ■ método de partículas ■ estabilidade em avaria ■ fluxo multifásico ■ MPS

Resumen

Este estudio llevó a cabo simulaciones numéricas de los procesos transitorios y acoplados del derrame de petróleo o inundación de agua y analizó la estabilidad de un buque petrolero dañado. El enfoque numérico basado no método Moving Particle Semi-Implicit (MPS) fue aplicado para determinar la dinámica de un modelo de dos dimensiones a escala y el flujo multifásico de petróleo y agua con la superficie libre. Los resultados se compararon con el *software* de análisis de estabilidad SStab, que proporcionó el ángulo final de adornación, y mostró un buen acuerdo. Además de la dinámica de derrame de petróleo y la inundación de agua, que proporcionan informaciones importantes, como el tiempo desde los daños hasta la inclinación final, los resultados del estudio también muestran los límites de la aproximación casi-estática.

palabras-clave: ■ análisis acoplados ■ derrame de petróleo ■ método de partículas ■ estabilidad con avería ■ flujo multifásico ■ MPS

Introduction

Vessel stability and oil leakage are of great concern when a crude oil carrier is damaged due to the threat to safety and environmental issues. Within this context, list angle assessments, oil leakage volume and dynamic effects or water flooding are pertinent topics in crude oil carrier design and operation.

Nowadays, several methods and computational tools can calculate the damaged stability; however, most are based on a hydrostatic approach and/or quasi-static assumption. As the restoring moment is affected by the free surface effect of the liquid inside the tank, the oil leakage or water flooding and their dynamic effects, the quasi-static approach is unable to give a reliable assessment principally where water flooding occurs. Even in cases of CFD based approaches, due to the fluid-solid interaction with complex geometry and multiphase flow, the detailed investigation of oil leakage including the coupled transient motions of the fluids and vessels is a challenge.

To this end, this study sought to carry out a coupled transient analysis of the oil leakage process and the damaged stability. A numerical method based on Moving Particle Semi-Implicit (MPS) method (Koshizuka and Oka, 1996) was adopted to model both the vessel motion and the oil-water multiphase flow with free surface.

For sake of simplicity, a two dimensional (2D) small scaled model is considered. The effects of ballast condition, the hull damage height and the liquid cargo filling ratio were considered in the analysis. The results were compared with the stability analysis software SStab, which provided the final list angle, related to the damage, and showed very good agreement. The following sections give a brief numerical model description, some validation analysis results, the study cases, results and discussions.

Numerical method

The governing equations of incompressible viscous flow that express the problem to be solved are:
continuity equation

$$\frac{D\rho}{Dt} = -\rho(\nabla \cdot \vec{u}) = 0 \quad (1)$$

and the *momentum* equation

$$\frac{D\vec{u}}{Dt} = -\frac{1}{\rho} \nabla P + \nu \nabla^2 \vec{u} + \vec{g} + \frac{\vec{\sigma}}{\rho} \quad (2)$$

Where:

ρ = density;

u = velocity;

P = pressure;

ν = kinematic viscosity;

σ = surface tension;
 g = gravity.

The Moving Particle Semi-implicit (MPS) is a Lagrangian meshless method, in which the space domain is discretized in particles, and all the differential operators are obtained from a particle interaction model based on the weight function given by:

$$w(r) = \begin{cases} \frac{r_e}{r} - 1, & (r < r_e) \\ 0, & (r > r_e) \end{cases} \quad (3)$$

Where:

r = distance between two particles;

r_e = the effective radius, which limits the region where the interaction between particles occurs.

Considering a scalar function ϕ , the gradient vector and the Laplacian of the function at a particle i are determined taking into account the neighboring particles j within the range r_e . They are given by equations 4 and 5, respectively:

$$\langle \phi \rangle_i = \frac{d}{pnd^0} \sum_{i \neq j} \left[\frac{(\phi_j - \phi_i)}{|\vec{r}_j - \vec{r}_i|^2} (\vec{r}_j - \vec{r}_i) w(|\vec{r}_j - \vec{r}_i|) \right] \quad (4)$$

$$\langle \nabla^2 \phi \rangle_i = \frac{2d}{pnd^0 \lambda} \sum_{i \neq j} [(\phi_j - \phi_i) w(|\vec{r}_j - \vec{r}_i|)] \quad (5)$$

Where:

d = number of spatial dimensions;

pnd = particle number density. λ is calculated by:

$$\lambda = \frac{\sum_{i \neq j} |\vec{r}_j - \vec{r}_i|^2 w(|\vec{r}_j - \vec{r}_i|)}{\sum_{i \neq j} w(|\vec{r}_j - \vec{r}_i|)} \quad (6)$$

and the particle number density (pnd) is proportional to the fluid density and it is given by:

$$pnd = \sum_{i \neq j} w(|\vec{r}_j - \vec{r}_i|) \quad (7)$$

and pnd^0 is the initial value of pnd .

The MPS method adopts a semi-implicit algorithm. Except the pressure gradient term, the right hand side of the Navier-Stokes equation is calculated explicitly to estimate velocity and position. After that, the Poisson's equation of pressure is solved implicitly at $(t + \Delta t)$. The Poisson's equation is given by:

$$\langle \nabla^2 P \rangle_i^{t+\Delta t} = -\frac{\rho}{\Delta t^2} \frac{pnd_i^* - pnd^0}{pnd^0} \quad (8)$$

Where:

pnd^* = particle number density calculated using the estimated position of the particles.

pnd^* is kept as pnd^0 to ensure the condition of incompressibility. The left hand side term of equation 8 can be discretized using the Laplacian model, leading to a system of linear equations.

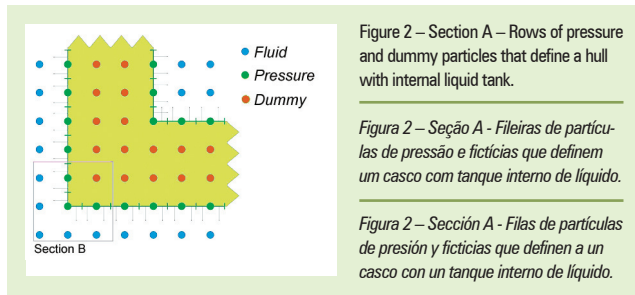
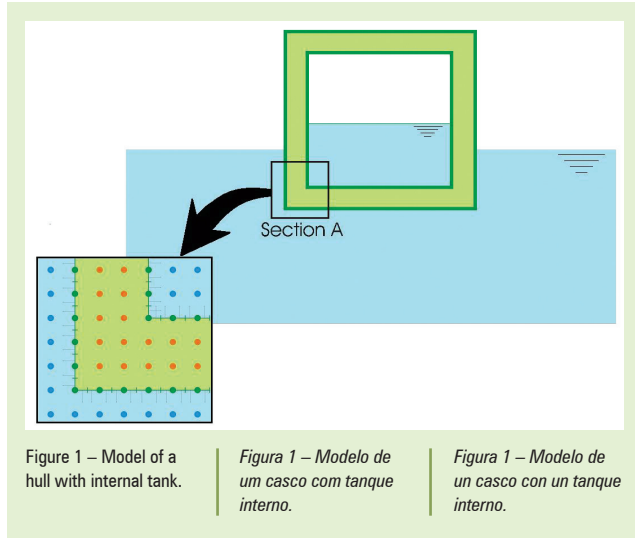
For the present two-dimensional analysis, r_e was set to $2.1l_0$, where l_0 is the initial distance between particles, to calculate pressure gradient and the particle number density. r_e is set to be $4.0 l_0$ for cases involving the Laplacian operator.

When the particle number density is smaller than $\beta \cdot pnd$, it is considered to be on the free surface. The pressure of all free surface particles is set to zero. According to Koshizuka and Oka (1996), β may vary between 0.80 and 0.99.

To calculate the surface tension $\vec{\sigma}$ in the free surface and in the water-oil interface, the inter-particle potential force model proposed by Kondo *et al.* (2007) is used.

In MPS, rows of different types of particles are used to describe the rigid wall geometry. Pressure is calculated in the first row in contact with fluids. The rows of particles that have no contact with fluids are formed by dummy particles used to guarantee the correct particle number density calculation, but in which the calculation of pressure is not necessary.

In the studied case of the floating body with an inner tank, the liquid pressure calculation on the outside of the hull must not affect the calculation of the pressure inside the hull, and vice-versa. Therefore, for r_e equal to $2.1l_0$, it is necessary put at least two dummy particle rows between the pressure particle rows that define the hull and inner tank geometry, as shown in figures 1 and 2.



Force and moment acting on the hull are calculated by integrating the pressure on both external and internal sides of the body. The wall elementary area is defined as the half distance between a hull particle and one of its neighbor particles. Each area has its normal orientated to the fluid side. Figure 3 shows an example of hull particles, their elementary areas and normal vectors.

The force on the hull and the moment applied at the center of gravity are as follows:

$$F = \sum_i P_i \cdot (S_{i1} \cdot \vec{n}_{i1} + S_{i2} \cdot \vec{n}_{i2}) \quad (9)$$

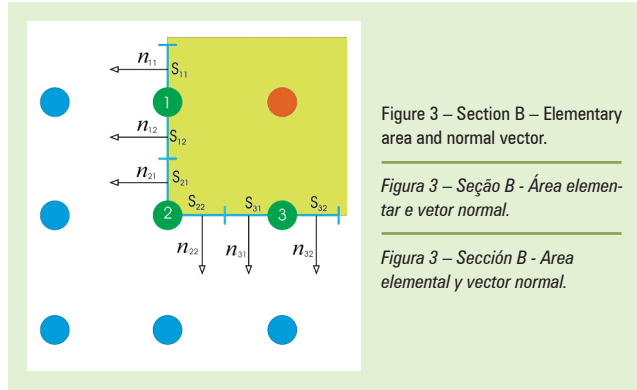
$$M = \sum_i P_i \cdot (S_{i1} \cdot \vec{n}_{i1} + S_{i2} \cdot \vec{n}_{i2}) \times (\vec{r}_i - \vec{r}_{CG})$$

Where:

S_{i1} and S_{i2} = dimension of the two elementary areas of particle i ;

P_i = pressure of particle i ;

\vec{n}_{i1} and \vec{n}_{i2} = normal vectors of S_{i1} and S_{i2} , respectively;



\vec{r}_i = position vector of particle i ;

\vec{r}_{CG} = position vector of center of gravity of the floating body.

With the force and the moment calculated by equation 9, the dynamics of the floating body can be obtained by:

$$m \frac{d^2 \vec{r}_{CG}}{dt^2} = F$$

$$I \frac{d^2 \theta}{dt^2} = M \quad (10)$$

Where:

m and I = mass and inertia of rigid body respectively;

θ = roll angle.

Validation

To confirm the numerical approach effectiveness in the fluid leakage problem, some simple case simulations were carried out by the authors. Among the validation studies, we can mention Silva *et al.* (2008) that investigated the water tank leakage and flooding, as well as the dynamics of a floating body in waves and the coupled motion of sloshing and a vessel in waves. Further basic tests on fluid-solid interaction such as a floating body free heave and roll motions with and without elastic connection were also performed by the authors (Tsukamoto *et al.*, 2009). All of them show good agreement with the analytical and experimental results.

Case studies

The damaged hull dynamics simulations after the break-

down were carried out using a 2D numerical model whose main characteristics are described in table 1. Two ballast conditions were considered: without ballast and with a ballast of 15.0kg.

Property	Without ballast (B0)	With ballast (B15)
Beam (m)	0.415	0.415
Depth (m)	0.325	0.325
Mass (kg/m)	25.109	40.109
Inertia (Kgm ² /m)	0.801	1.088
TCG (m)	0.0	0.0
VCG (m)	0.129	0.094

Table 1 – The main properties of the hull.

Tabela 1 – As características principais do casco.

Tabla 1 – Las características principales del casco.

As shown in figure 4, the scaled model has two internal tanks. The wall thickness is 0.02m except in center, where it is 0.025m, and the bottom, where the thickness is 0.055m to model the double bottom. There is a fixed 0.05m opening for the oil leakage.

To minimize the wave reflection generated by the hull dynamic motion, 0.8m beaches were modeled in both towing tank extremities with approximately 30 degree slopes. Squares of 3x3 particles were fixed close to the beaches. In the numerical simulations, a towing tank with total width of 2.7m and depth of 0.40m was used, as shown in figure 5.

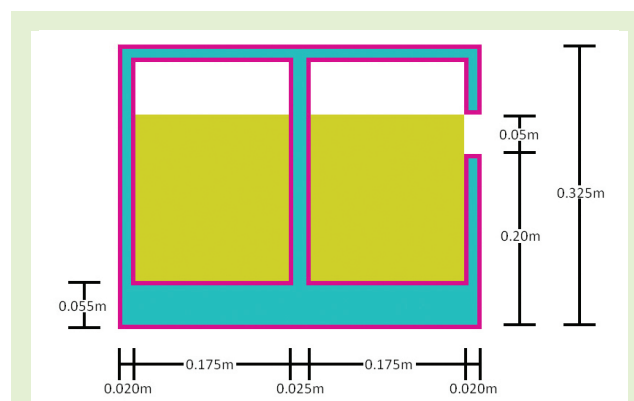


Figure 4 – Cross-section of the model showing the opening height 0.20m above the keel, and the internal tank filling ratio is 75%.

Figura 4 – Seção transversal do modelo mostrando a abertura com 0,20m de altura acima da quilha, e o tanque interno com a taxa de enchimento de 75%.

Figura 4 – Sección transversal del modelo que muestra la apertura con 0,20m de altura por encima de la quilla, y el tanque interna con una tasa lleno de 75%.

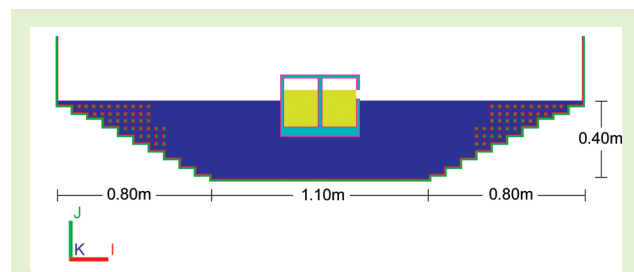


Figure 5 – Cross-section of the towing tank.

Figura 5 – Seção transversal do tanque de provas.

Figura 5 – Sección transversal del canal hidrodinámico.

The analyzed cases are shown in table 2. For both ballast conditions, three different opening locations and three filling levels inside the tanks were considered. The water and oil properties are given in table 3.

Case denomination		Filling ratio (%)	Damage height above the keel (m)
Without ballast (B0)	With ballast (B15)		
B0_75%_020	B15_75%_020	75	0.20
B0_75%_014	B15_75%_014	75	0.14
B0_75%_010	B15_75%_010	75	0.10
B0_45%_014	B15_45%_014	45	0.14
B0_45%_010	B15_45%_010	45	0.10
B0_25%_010	B15_25%_010	25	0.10

Tabela 2 – The case studies.

Table 2 – Os casos de estudo.

Tabla 2 – Los casos de estudio.

Property	Water	Oil
Density (kg/m ³)	1000.0	900.0
Viscosity (m ² /s)	1.0x10 ⁻⁶	5.0x10 ⁻⁵
Surface Tension Coefficient (N/m)	0.072	0.026

Table 3 – The properties of the water and oil.

Tabela 3 – As propriedades da água e do óleo.

Tabla 3 – Las propiedades del agua y el petróleo.

The simulations were carried out by using distance between particles of 0.005 m. The time step was 0.0005 s and simulation times up to 10.0 s were used. In a typical case there are about 30000 particles.

Results and discussions

Figure 6 shows the snapshots obtained from the MPS simulation with 75% filling and an opening 0.10m above the keel (B0_75%_010). The transient analysis in this simulation shows that, beside the hull roll motion, a leakage induced

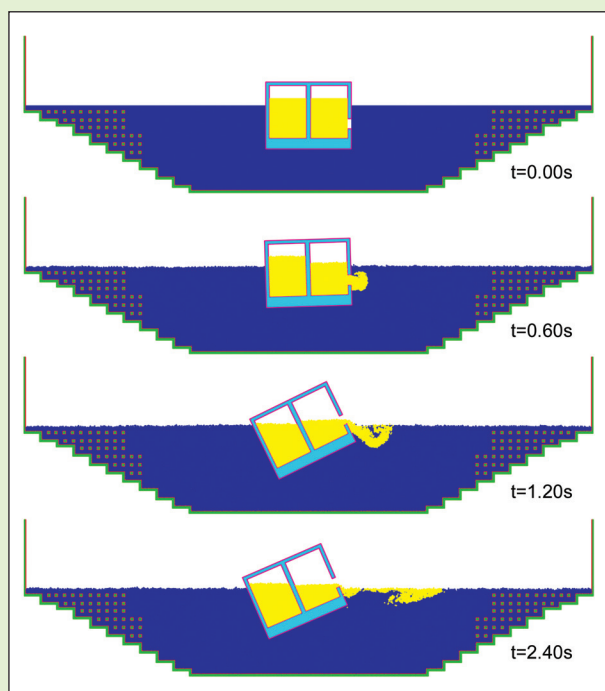


Figura 6 – Snapshots of the case B0_75%_010 simulation.

Figure 6 – Sequência da animação da simulação do caso B0_75%_010.

Figura 6 – Instantáneas de la simulación del caso B0_75%_010.

drift motion occurs at the process start, when a relatively large volume of oil is suddenly released. When the opening is higher, as in the case B0_75%_020, the drift motion becomes negligible because there are almost no dynamic effects induced by the relatively small oil leakage volume.

The snapshots of figure 6 show a nearly 30 degree list angle is reached in about 2 seconds following the oil release. This short time is expected considering the adopted model characteristics: the reduced model dimensions with a relatively large opening. Also, the 2D analysis means an unlimited opening in longitudinal direction. This is a hypothetical condition that leads to a relatively large initial oil volume being released at once, being very different from a real situation. Thus, it must be emphasized all the presented results should be interpreted bearing these differences in mind. A complete 3D analysis should be done instead of simply extrapolating the 2D results to the actual situations.

The final equilibrium list angle confirmation was carried out with SStab (Coelho and Nascimento, 2003). SStab is the official stability analysis code adopted by Petrobras, and uses the hydrostatic theory to calculate the stability of floating bodies with and without free-surface effects, and free to pitch and heave. To model the 2D problem, a 3D model of $B/L = 1/100$ with constant cross section and without trim is used in the SStab calculations.

Although SStab is able to provide an estimate the final list angle through a quasi-static approach, it is unable to take into account the dynamic effects due to oil leakage or water flooding. Therefore, the final list angle provided by SStab is determined by using the volume obtained by MPS simulation.

Figure 7 provides the roll motion time series obtained by MPS simulation and the final list angle obtained by SStab for the case B0_75%_014. The transient motions calculated by MPS show damped motion oscillations after a quick inclination from the initial position.

The motion damping shows the effectiveness of the beaches at both ends of the towing tank: when only one end was beached, the wave reflection from the wall caused irregular residual motions and affected the list angle accuracy.

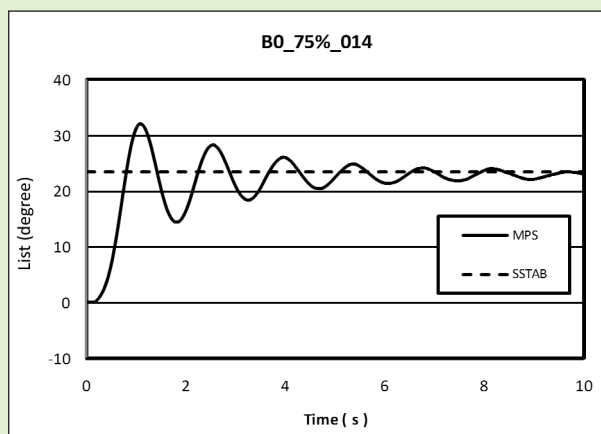


Figure 7 – Time history of the list angle obtained by MPS transient analysis and list angle obtained by the SSTab hydrostatic analysis for internal tank with 75% filling and opening height 0.14m (BO_75%_014).

Figura 7 – Série temporal do ângulo de adernamento obtido pela análise transiente de MPS e o ângulo de adernamento obtido pela análise hidrostática de SSTab para o tanque interno com 75% de enchimento e a altura da abertura em 0,14m (BO_75_014%).

Figura 7 – Evolución temporal del ángulo de la inclinación, obtenido por análisis transitorio de MPS y el ángulo de la inclinación obtenido por el análisis hidrostático de SSTab del tanque interno con 75% lleno y la altura de la apertura en 0,14m (BO_75_014%).

In the figures, the computed time series converge to a mean value, which is nearly 23.0° . This value agrees very well with the final list angles of 23.4° obtained with SSTab.

A comparison of the list angle snapshot obtained by MPS at 10.0s and the graphic output from SSTab in the BO_45%_010 case is given in figure 8. The images show that in this case both the list angle and the draught obtained by MPS agree well with that obtained with SSTab.

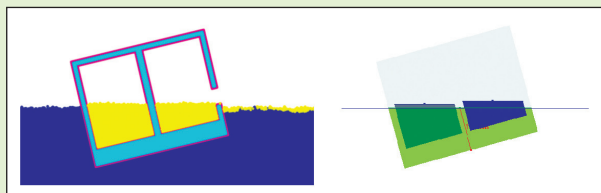


Figura 8 – Comparison between the final list angles obtained by MPS (left) and by SSTab (right) for BO_45%_010 (45% filling and opening height 0.10m).

Figura 8 – Comparação entre os ângulos finais de adernamento obtidos por MPS (esquerda) e por SSTab (direita) para BO_45%_010 (45% de enchimento e altura da abertura de 0,10m).

Figura 8 – Comparación entre los ángulos finales de la inclinación obtenidos por MPS (izquierda) y por SSTab (derecha) para BO_45%_010 (45% lleno y la altura de la apertura de 0,10m).

The list angles obtained by MPS and SSTab are compared in figure 9 for 45% and 75% filling and 0.10m, 0.14m and 0.20m opening heights. In the case of 45% filling and 0.20m height no leakage occurred, and in the case of 25% filling and 0.10m height water flooding occurred, so these two cases were not considered. Here, as with the previous SSTab results, the MPS simulation leaked volume is used in the SSTab calculation. The comparison shows the relatively small discrepancies between the final list angles obtained by MPS and SSTab. The discrepancies are minimal in the cases of 75% filling, and increase when the filling ratio decreases. This behavior seems to be related to the discretization adopted by the simulation: the discrepancies increase when the 'oil particles' quantity released from the internal tank is drastically reduced, and a higher resolution is required to model the smaller change of leakage volume.

The oil leakage volume calculated by MPS is given in figure 10, together with the estimated leakage using SSTab through the quasi-static approach. The figure 10 vertical axis is the leaked oil volume in relation to the volume of one internal tank. The comparison between the results shows very good agreement. Despite the dynamic effects such as roll and drift motions, the discrepancies are smaller than 1.0% of the internal tank volume, except in the BO_75%_020 case, where the discrepancy is about 2.5%.

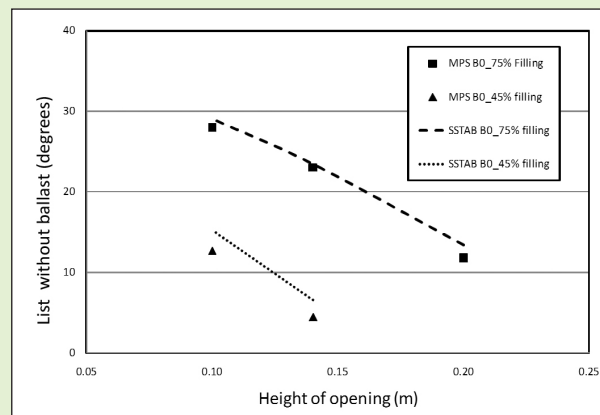


Figura 9 – Comparison of the list angle obtained by MPS and by SSTab for 45% and 75% filling and opening height 0.10m, 0.14m and 0.20m without ballast.

Figura 9 – Comparação do ângulo de adernamento obtido pelo MPS e pelo SSTab por 45% e 75% de enchimento e a altura da abertura de 0,10m, 0,14m e 0,20m, sem lastro.

Figura 9 – Comparación del ángulo de la inclinación obtenido por MPS y por SSTab por 45% y 75% llenos y la altura de la apertura en 0,10m, 0,14m y 0,20m, sin lastre.

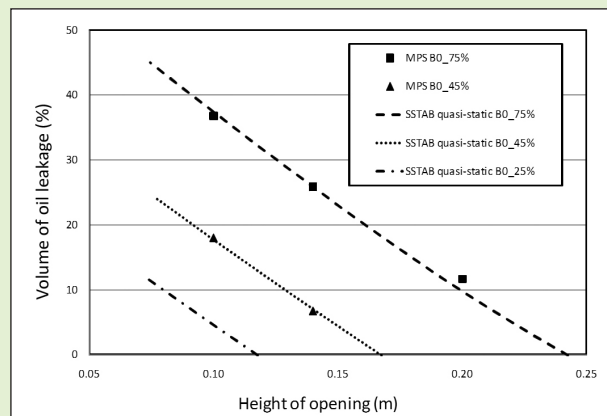


Figure 10 – Oil leakage obtained by MPS and by quasi-static calculation using SSTab for 45% and 75% filling and opening height 0.10m, 0.14m and 0.20m.

Figura 10 – Derramamento de óleo obtido por MPS e pelo cálculo quase-estático usando SSTab por 45% e 75% de enchimento e altura de abertura de 0,10m, 0,14m e 0,20m.

Figura 10 – Derrame de petróleo obtido por MPS y el cálculo cuasi-estático utilizando SSTab por 45% y 75% llenos y la altura de la apertura en 0,10m, 0,14m y 0,20m.

Also, for filling ratio of 25% (BO_25%) shown in figure 10, the quasi-static approach predicts an oil leakage when the opening height is 0.10m. This occurs because one of the quasi-static approach key assumptions is a very small opening. However, as illustrated in figure 11, the snapshots of the BO_25%_010 simulation show that, instead of oil leakage, water flooding occurs. To clarify how this unexpected situation by quasi-static approach occurs, figure 11 shows only the process beginning: when the oil and water surfaces and the opening are almost at same level, besides a very small oil leakage, an increasing volume of water floods into the tank. After achieving a negative list angle at $t=2.4$ s, water quickly floods into the tank and the final list angle reaches -45° , in a sequence similar, but slower, than shown in figure 12. The final flooded water volume calculated by MPS is as large as 65.3% of one internal tank volume. This huge discrepancy shows the validity limit of the quasi-static approach.

According to the simulation results, instead of oil leakage, water flooding occurs in all of the cases with ballast. The animation snapshots shown in figure 12 are from the simulation with 25% filling and the opening 0.10m above the keel (B15_25%_010). As the tank void space is relatively large in this case, a huge amount of water floods into the tank causing fast heeling of the hull. The motion is so violent that a wave can be observed in $t=1.2$ s. Finally, the flooding water,

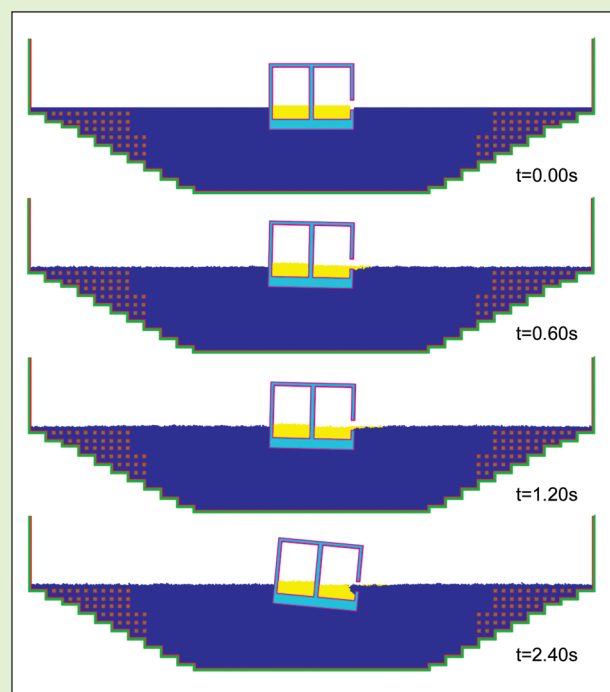


Figure 11 – Snapshots of the case BO_25%_010 simulation showing the water flooding instead of oil leakage.

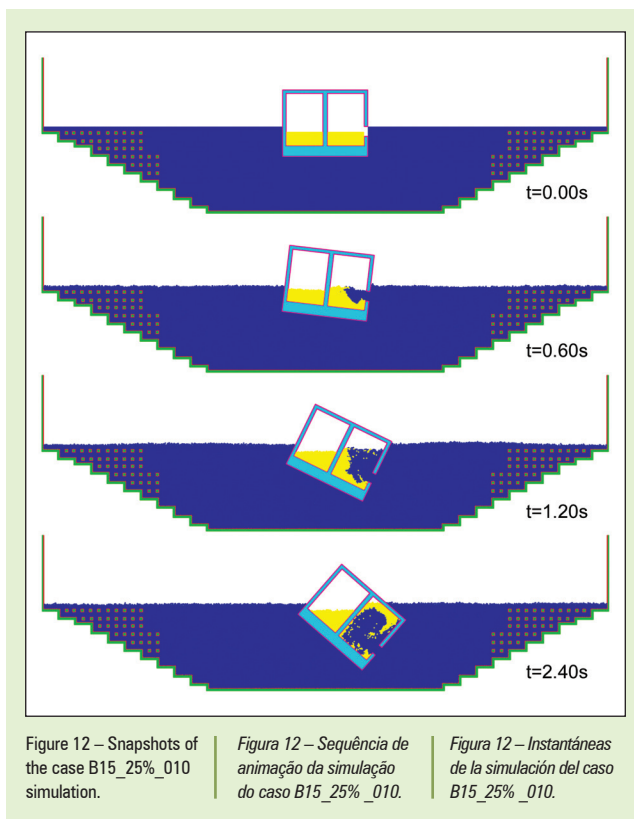
Figura 11 – Sequência da animação da simulação do caso BO_25%_010 mostrando a água inundando em vez de o óleo vazando.

Figura 11 – Instantáneas de la simulación del caso BO_25%_010 que muestra el agua inundando en vez del petróleo saliendo.

whose density and surface tension are greater than oil, washes the tank bottom and inner side walls and pushes the oil to the tank ceiling.

The flooded water volume obtained by MPS simulation is provided in figure 13. The figure 13 vertical axis is the flooded water volume in relation to the volume of one internal tank. As the presence of air is neglected in this modeling, the flooding volume depends on the void space inside the tank. As illustrated in figure 13, when the filling ratio increases, the void space is smaller and the flooded water volume reduces as well as the final list angle. Therefore, if flooding occurs, lower filling conditions will be more dangerous. It is also interesting to note that according to the numerical results, the flooding volume and the final list angle are independent of the opening height.

Finally, the mean error of the displaced water volume is less than 3% in all the analyzed cases, except the BO_45%_010 case, where the error is about 4.5%.



Concluding remarks

This study investigated the dynamics of oil leakages and the damaged stability of a crude oil carrier. Numerical simulations based on the MPS (Moving Particle Semi-Implicit) method were carried out taking into account the coupling between the damaged hull and the multiphase flow.

The numerical simulations of the transient motion of those cases without ballast show that the drift motion induced by the leakage may occur at the process start when a relatively large volume of oil is released. From the comparison between the final list angles with those obtained from SSTab, which is a static stability code, it is clear the numerical approach is very effective to predict the dynamic behavior of a damaged oil carrier. This was mapped from breakdown to final list, and included damped roll motion and its response time, which may be important to safeguard environmental issues. Concerning the numerical results accuracy, it increases in cases where the filling ratio is large and the height of the damage is low down.

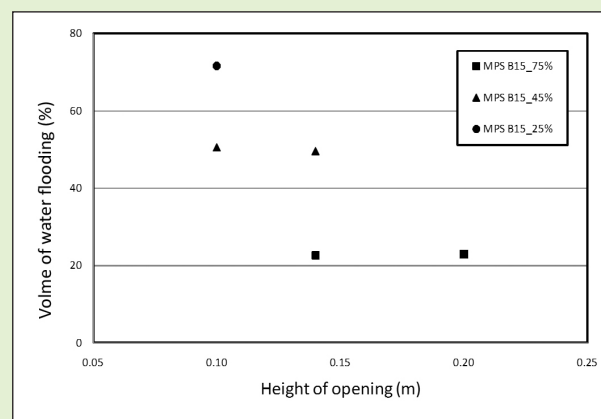


Figure 13 – Volume of flooded water obtained by MPS for 25%, 45% and 75% filling and opening height 0.10m, 0.14m and 0.20m with ballast.

Figure 13 – Volume de água inundada obtido por MPS para 25%, 45% e 75% de preenchimento e a altura da abertura em 0,10m, 0,14m e 0,20m com lastro.

Figura 13 – Volumen del agua inundada obtenido por MPS para 25%, 45% y 75% lleno y la altura de la abertura en 0,10m, 0,14m, y 0,20m con lastre.

Also, although the complete oil spillage simulation was not realized because the thin oil film formation would demand a very large number of particles beyond the study's scope, the volume of leakage was computed. The comparison between computed oil volume with that obtained by quasi-static approach shows the validity limit of the latter.

For those cases with ballast, water flooding occurs, and the simulation results show the flooded water volume is inversely proportional to the filling ratio. Also, the opening height has no significant effect on the final list and flooded volume.

Finally, for the sake of simplicity, 2D modeling was carried out to investigate the complex fluid-solid interaction phenomena. This is a hypothetical situation in which the dimension of the damage is much larger than actual cases. Therefore, instead of simply extrapolating the 2D results to the real situations, further complete 3D analyses should be done. Furthermore, future studies on the effects of the air inside the tank are also required.

Acknowledgments

The authors would like to express their gratitude to Petrobras for their financial support for the research.



Referências Bibliográficas

■ COELHO, L. C. G.; NASCIMENTO, A. A. **SSTab User's Manual**. Rio de Janeiro: PUC; Tecgraf, 2003.

■ KOSHIZUKA, S.; OKA, Y. Moving-particle semi-implicit method for fragmentation of incompressible fluid. **Nuclear Science and Engineering**, Illinois, v. 123, n. 3, p. 421–434, July 1996.

■ KONDO, M.; KOSHIZUKA, S.; TAKIMOTO, M. Surface tension model using inter-particle potential force in Moving Particle Semi-implicit method. **Transactions of JSCES**, Tokyo, v. 2007, paper n. 20070021, Aug. 2007.

■ SILVA, G. E. R.; TSUKAMOTO, M. M.; MEDEIROS, H. F.; CHENG, L. Y.; NISHIMOTO, K.; SAAD, A. C. Validation study of MPS (Moving Particle Semi-implicit Method) for sloshing & damage stability analysis. In: INTERNATIONAL CONFERENCE ON OFFSHORE MECHANICS AND ARCTIC ENGINEERING (OMAE 2008), 27., 2008, Estoril, Portugal. **Proceedings...** New York: ASME, 2008. Paper n. OMAE2008-57460.

■ TSUKAMOTO, M. M.; CHENG, L. Y.; NISHIMOTO, K. Numerical Study of the Motions in Shallow Water Waves of Floating Bodies Elastically Linked to Bottom. In: INTERNATIONAL CONFERENCE ON OCEAN, OFFSHORE AND ARCTIC ENGINEERING (OMAE 2009), 28., 2009, Honolulu, Hawaii. **Proceedings...** New York: ASME, 2009. Paper n. OMAE2009-80126.

Autores



Liang-Yee Cheng

Universidade de São Paulo (USP)
Escola Politécnica
e-mail: cheng.yee@poli.usp.br



Diogo Vieira Gomes

Universidade de São Paulo (USP)
Escola Politécnica
e-mail: diogogomes@usp.br

Liang-Yee Cheng graduou-se em Engenharia Naval, na Universidade de São Paulo em 1989 e recebeu seu título de Mestre e Doutor em Engenharia, pela *Yokohama National University*, em 1992 e 1995, respectivamente. Em 1995, juntou-se ao *Tokyo Research Center*, da *Ishikawajima Harima Heavy Industry*, como estagiário com uma bolsa de AOTS. Em 1996, ingressou no Departamento de Engenharia de Construção Civil, na Escola Politécnica da USP, como professor assistente doutor. Suas pesquisas estão focadas na simulação numérica da hidrodinâmica não linear e modelagem fuzzy dos problemas de projeto de engenharia.

Diogo Vieira Gomes é um estudante de graduação na Engenharia Civil da Escola Politécnica da Universidade de São Paulo. Seus interesses de pesquisa são: Simulação numérica baseada em métodos de partículas e métodos de elementos finitos. Interessado na modelagem dos problemas de engenharia civil e naval juntou-se ao laboratório Tanque de Provas Numérico (TPN), em 2009.



Kazuo Nishimoto

Universidade de São Paulo (USP)
Escola Politécnica
e-mail: knishimo@usp.br

Kazuo Nishimoto graduou-se em Engenharia Naval e Oceânica pela Universidade de São Paulo, em 1979. Obteve o título de Mestre em Engenharia Naval e Oceânica pela *Yokohama National University* do Japão, em 1982 e título de Doutor em Engenharia Naval e Oceânica pela *University of Tokyo* do Japão, em 1985. Fez pós-doutorado pela *University of Tokyo*, em 1991 e pela *University of Michigan*, em 1997. É professor titular da Universidade de São Paulo. Atuou em diversos projetos de desenvolvimento na área naval e oceânica, principalmente, relacionados a sistemas *offshore* e navios militares. Coordenou os desenvolvimentos de MonoBR e FPSOBR, principais sistemas flutuantes de produção que estão sendo considerados como sistemas em águas ultraprofundas, junto com a Petrobras. Desenvolveu os simuladores *Dynasim* e Tanque de Provas Numérico (TPN) para análise de sistemas de flutuantes ancorados e com dutos (*risers*) acoplados. Em 2009, inaugurou o laboratório com sistema computacional do Galileu (rede temática de computação científica e visualização) de 55T flops e um tanque físico com gerador e absorvedor de ondas ativo.